NJC

ROYAL SOCIETY OF CHEMISTRY

COMMUNICATION

View Article Online
View Journal

Cite this: DOI: 10.1039/d6nj00620e

Received 17th February 2026,
Accepted 22nd May 2026

DOI: 10.1039/d6nj00620e

rsc.li/njc

Photocontrolled immunotherapy: a BODIPY-caged MSA-2 for spatiotemporal activation of STING with visible light

Karan Arora, †*[a] Alexandra E. Lee,†[b] Neil C. Chada, [bc] Jacob A. Schulman[b] and John T. Wilson *[abd]

The STING pathway is a promising target for cancer immunotherapy, but systemic activation by small-molecule agonists can cause adverse effects. We report a visible light-activatable STING agonist, BODIPY-MSA-2, enabling precise, light-dependent uncaging and restoration of STING activity *in vitro*, with potential to enable spatiotemporal control of immunostimulation.

The STING (stimulator of interferon genes) pathway is a central mediator of cytosolic DNA sensing[1,2] and plays an important role in antitumor immunity by promoting a type I interferon response.[3–6] Non-nucleotide, small molecule STING agonists, such as MSA-2, have emerged as promising immunotherapeutic agents.[7,8] However, systemic administration of STING agonists can lead to widespread inflammation,[9] limiting clinical application.[10,11] Additionally, chronic activation of the STING pathway is associated with autoimmune[12,13] and metabolic diseases.[9,14,15]

To address this, spatiotemporal control of STING activation is desirable. Photopharmacology—the use light to modulate biological activity—offers an attractive solution by enabling precise control over drug activation in target tissues.[16,17] Recent efforts to implement photopharmacology to improve STING pathway control have been successful.[18,19] For example, diBSP01, a dimerized form of an MSA-2 analogue, successfully enhanced STING protein binding and pathway activation; its photocaged form, caged with diethylaminocoumarinyl-4-methyl (DEACM), exhibited masked activity in the absence of irradiation in a zebrafish xenograft model.[20] Non-dimerized MSA-2 was also used as the starting molecule for photocaging, with its photocaged form equipped with tumor-cell targeting *via* carbonic anhydrase IX (CAIX), a protein commonly expressed on the surface of cancerous cells.[21] Furthermore, photocaged STING agonists have shown success in enhancing dendritic cell maturation and tumor antigen cross-presentation,[22] M1 macrophage polarization,[23] and sustaining a prolonged immune response. However, these technologies rely on uncaging at a specific wavelength which requires a specialized laser making translation more challenging, and thus, expanding this range to the full visible spectrum would allow for greater translatability.

Photocaging with chromophores such as BODIPY (boron-dipyrromethene), which release cargo in response to visible light, allows deeper tissue penetration with reduced toxicity[24] compared to ultraviolet (UV)-based systems.[25] Along with limited penetration,[26] prolonged exposure to UVA, a form of UV light, can lead to unwanted effects in epidermal and dermal immune cells, accelerated skin aging, and an increased risk of carcinogenesis.[27] Additionally, BODIPY proved advantageous in biomedical applications due to its high chemical and photostability,[24,28] its invariance in environments with varying pH and polarity.[29,30]

In this study, we report the development of a visible-light–activatable STING agonist generated by covalently linking the small-molecule agonist MSA-2 to a BODIPY-based photocaging group, rendering the compound inactive until light exposure. The BODIPY chromophore enables efficient photolysis under visible-light irradiation, at which point BODIPY–MSA-2 is uncaged to release bioactive MSA-2. The liberated MSA-2 can then bind STING on the endoplasmic reticulum membrane and activate downstream IRF-mediated interferon signalling. We characterize the synthesis, photochemical properties, and biological activity of this photoactivatable STING agonist and demonstrate robust light-dependent STING activation in immune cells. This strategy enables precise, spatiotemporal control of innate immune activation and holds promise for minimizing off-target or systemic immune responses *in vivo*. Notably, BODIPY-based photocages are particularly advantageous because they enable the release of carboxylate-containing

[a] *Department of Chemical and Biomolecular Engineering, Vanderbilt University, Nashville, Tennessee 37212, USA. E-mail: john.t.wilson@vanderbilt.edu, karan.arora@vanderbilt.edu; Tel: +1-615-322-6406*
[b] *Department of Biomedical Engineering, Vanderbilt University, Nashville, Tennessee 37240, USA*
[c] *Medical Scientist Training Program, School of Medicine, Vanderbilt University, USA*
[d] *Vanderbilt Ingram Cancer Center, Nashville, Tennessee 37232, USA*
† Co-first author.

molecules using visible light, circumventing the need for high-energy UV excitation required by most conventional photocaging groups.[31,32]

Masking the free carboxylic acid functionality on MSA-2 with a BODIPY moiety was anticipated to not only enable controlled photoactivation under mild light conditions but also enhance the compound's membrane permeability. To confer light sensitivity to MSA-2, we identified the carboxylic acid in MSA-2 as suitable for coupling to a hydroxyl-functionalized BODIPY photocage, effectively photo-caging the STING-binding capacity of MSA-2. A custom BODIPY-based photocage with a red-shifted absorption maximum (~530–650 nm) was synthesized and conjugated to MSA-2 *via* an ester linkage (Fig. 1). The resulting BODIPY-MSA-2 compound was purified by column chromatography and confirmed by high resolution mass spectrometry (HRMS), high-performance liquid chromatography (HPLC) and nuclear magnetic resonance (NMR) spectroscopy.

The synthesis of the target BODIPY-MSA-2 analogue (**1**) was accomplished *via* esterification. The coupling of BODIPY-Me_2-OH[33,34] with the carboxylic acid MSA-2[8] was performed *via* a Steglich esterification using EDC as the coupling reagent and DMAP as the catalyst in THF at room temperature overnight. This reaction yielded the desired analogue, BODIPY-MSA-2, as an ester conjugate, which is purified by column chromatography and characterized by HRMS and NMR spectroscopy.

BODIPY-MSA-2 exhibits a pronounced absorption band in the visible region of the spectrum (approximately 500–550 nm), arising from the characteristic electronic transition of the BODIPY chromophore. Excitation at these wavelengths enables photochemical activation using visible light, which offers improved tissue penetration and reduced phototoxicity relative to UV-based photocaging strategies. Upon visible-light irradiation, the BODIPY photocage undergoes rapid and efficient photolytic cleavage through an excited-state intramolecular charge transfer mechanism, resulting in the quantitative release of free MSA-2. The photo-uncaging process was comprehensively characterized by HPLC and NMR spectroscopy, which confirmed the disappearance of the caged precursor (compound **1**) and the concomitant formation of the liberated MSA-2 (Fig. 2A). These findings collectively indicate that the BODIPY caging strategy can provide a reliable and efficient platform for light-controlled activation of STING agonists in biological environments.

Photouncaging of compound **1** was further validated through detailed ^{1}H NMR spectroscopic analysis (Fig. 2B).

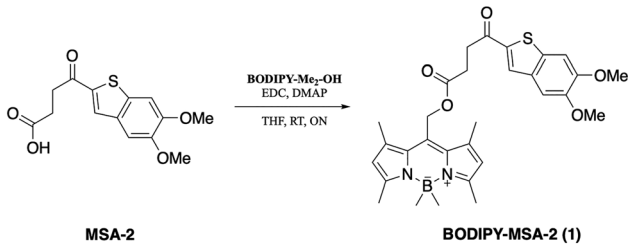

Fig. 1 Schematic representing the synthesis of BODIPY-MSA-2 (**1**).

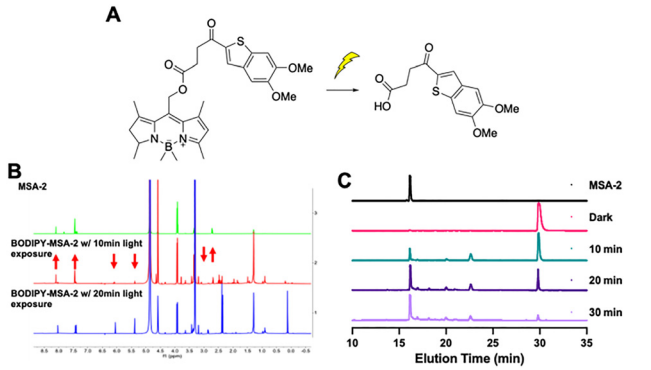

Fig. 2 (A) Schematic illustration of the release of MSA-2 on visible light irradiation. (B) ^{1}H NMR spectra of compound **1** in MeOD upon visible light irradiation at t = 0, 10, and 20 min. (C) Samples were prepared in DMSO : MeOH (5 : 1) and irradiated with visible light for 0, 10, 20, and 30 minutes, followed by HPLC analysis. The HPLC chromatograms revealed a progressive decrease in the peak corresponding to compound **1** (retention time: 29.8 min), accompanied by a concomitant increase in the peak corresponding to free MSA-2 (retention time: 16.8 min), confirming time-dependent photo-uncaging of MSA-2.

Compound **1** was dissolved in deuterated methanol (CD_3OD) and divided into three aliquots: one was maintained in the dark as a control, while the other two were exposed to visible light irradiation for 10 min and 20 min, respectively. The resulting NMR spectra were compared with that of MSA-2 to assess the extent of photolytic release.

In the dark control sample, characteristic aromatic proton signals of the caged compound were observed at δ 8.03, 7.43, and 7.40 ppm, each integrating for one proton, consistent with the aromatic protons of the MSA-2 moiety in its protected form. Additionally, the methylene protons adjacent to the ester linkage appeared as a distinct signal at δ 2.86 ppm, confirming the intact BODIPY-MSA-2 conjugate.

Upon irradiation, the spectrum showed time-dependent changes consistent with photochemical cleavage of the BODIPY cage. After 10 minutes of light exposure, the signals corresponding to the caged species began to diminish, and new resonances corresponding to free MSA-2 emerged. Following 20 minutes of irradiation, the transformation was nearly complete, as evidenced by the appearance of diagnostic aromatic proton peaks at δ 8.09 ppm (1H) and δ 7.44 ppm (2H), matching those of authentic MSA-2. Concomitantly, the methylene resonance shifted from δ 2.86 to 2.70 ppm, consistent with cleavage of the ester bond and liberation of free MSA-2.

Collectively, these NMR results, in agreement with the HPLC analysis, confirm efficient and time-dependent photouncaging of MSA-2 from compound **1** under visible-light irradiation. After confirming the photo release of MSA-2 further *in vitro* analysis was done to confirm the activity of MSA-2 released from the photo cage.

To validate the light-induced uncaging of compound **1** prior to conducting cell-based experiments, a solution of **1** was prepared in a DMSO : MeOH (5 : 1) solvent mixture and subjected to controlled visible-light irradiation for varying time intervals (0, 10, 20, and 30 min). Immediately following irradiation,

the reaction mixtures were analysed by HPLC to monitor the photolysis process (Fig. 2C). The chromatographic profile revealed a progressive decrease in the peak corresponding to the caged precursor **1** (retention time = 29.8 min), which diminished completely upon extended light exposure. Concurrently, a new peak corresponding to the released MSA-2 (retention time = 16.18 min) appeared and increased in intensity, confirming successful photouncaging. Additional peaks observed at 20.1 and 22.7 min were assigned to photoproducts derived from the BODIPY chromophore, consistent with the formation of known photooxidation or fragment byproducts. These results collectively demonstrate efficient and time-dependent photolytic release of MSA-2 from compound **1** upon visible-light irradiation.

The ability of photoirradiation to restore STING pathway activation of the photocaged agonist BODIPY-MSA-2 was evaluated *in vitro* using THP-1 Dual™ reporter monocytes, which express a luciferase reporter under control of interferon regulatory factor (IRF) elements, allowing for relative luminescence to be assessed as a measure of STING activation.

Non-irradiated cells treated with BODIPY-MSA-2 exhibited baseline activity indistinguishable from that of the BODIPY only control, indicating that the STING agonist was suppressed while the photocage remained intact. In contrast, photoactivated BODIPY-MSA-2 displayed a significant increase in IRF-driven luminescence, approaching the levels induced by unmodified MSA-2. EC_{50} values for BODIPY-MSA-2 and native MSA-2 were 6.8 μM and 7.8 μM, respectively, with photoirradiation (Fig. 3A and C). These values fall within a comparable range, indicating similar potency and immune activation.

Importantly, cell viability assays demonstrated comparable compound toxicity across all three groups under both photoactivated and dark conditions, indicating that the recovered immune activity resulted from photochemical uncaging, rather than any chances due to light exposure. Although both BODIPY-MSA-2 and unmodified MSA-2 exhibited some cytotoxicity, cell viability remained high (>75%) in the range where STING activation was observed. *In vitro* testing revealed that EC_{50} values without light exposure for BODIPY-MSA-2, unmodified MSA-2, and BODIPY were 111.536 μM, 85.9 μM, and 232.4 μM, respectively (Fig. 3B).

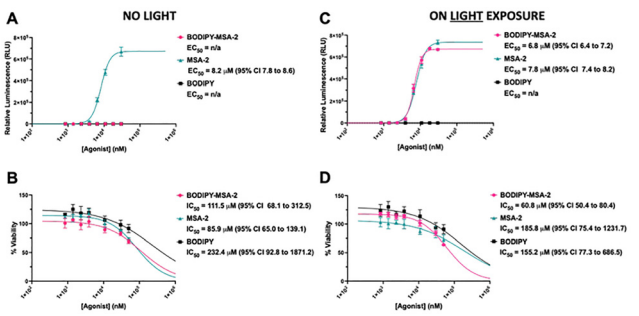

Fig. 3 (A) QUANTI-Luc™ dose–response curve showing relative luminescence vs [agonist] without any light exposure (B) cell viability curve of THP1-Dual™ cells in response to agonists without any light exposure (C) QUANTI-Luc™ dose–response curve showing relative luminescence vs [agonist] after light exposure (D) cell viability curve of THP1-Dual™ cells in response to agonists after light exposure.

IC_{50} values after light exposure for BODIPY-MSA-2, unmodified MSA-2, and BODIPY were 60.8 μM, 185.8 μM, and 155.2 μM, respectively (Fig. 3D). Collectively, these results confirm that BODIPY-MSA-2 remains functionally inert under dark conditions and can be reactivated *in vitro* through brief photoirradiation, providing control over STING pathway activation.

We developed a visible-light activatable STING agonist by covalently caging the small-molecule STING agonist MSA-2 with a BODIPY photocage, generating a construct that remains pharmacologically inert in the absence of light but rapidly restores bioactivity upon visible-light irradiation. This platform establishes a modular strategy for irreversible, non-invasive control of STING activation, providing a powerful tool for precision immunotherapy.

While past approaches demonstrated successful photocontrolled STING agonism with coumarin-based photocaging groups, such as by using 7-(diethylamino)-4-(hydroxymethyl) coumarin (DEACM) to photocage MSA-2 and its analogues,[35,36] the overall efficiency of photo-release is limited by chemical stability and photolysis quantum yields. While coumarin-based groups show high chemical stability, they are limited in their sensitivity to irradiation;[37] BODIPY-based photocaging groups exhibit high chemical stability and can resist hydrolysis under ambient light conditions, reflecting high photochemical stability and photolysis quantum yields.[37] Motivated by these properties, we employed BPDIPY caging of MSA-2 to achieve light-triggered STING activation.

A significant challenge associated with photoactivation in biological systems is the generation of reactive oxygen species (ROS), arising from the energy transfer between the photocage and molecular oxygen,[38] which can lead to cell death[39] through apoptosis[40] and necrosis.[41,42] While the BODIPY scaffold was chosen for its low phototoxicity relative to other UV-activated chromophores,[19] low-intensity irradiation with visible light can still produce peroxides and other ROS that influence cell viability, consequently impacting interpretations of immune activation and limiting the therapeutic dose. In preliminary experiments, photoirradiation of the culture media without ROS scavenging agents led to reduced cell viability. Beyond demonstrating proof-of-concept photoactivation, this study provides a foundation for achieving local and kinetically regulated immunomodulation *in vivo*, where innate immune pathways can be activated site-specifically with light exposure.

Author contributions

K. A. and J. T. W. conceived the project. K. A. and A. E. L. wrote the manuscript. N. C. C., J. A. S. designed experiments. K. A. synthesized the compounds. A. E. L., J. A. S., and N. C. C. performed the experiments. K. A., N. C. C. and A. E. L. analysed the data, and N. C. C. compiled the figures.

Conflicts of interest

There are no conflicts to declare.

Data availability

The data supporting this article have been included as part of the supplementary information (SI). Supplementary information including materials, methods, synthesis and charaterization details. See DOI: https://doi.org/10.1039/d6nj00620e.

Acknowledgements

This research was supported by grants from the National Institutes of Health (R01 CA245134 to J. T. W.). N. C. C. was supported by the Medical Scientist Training Program (MSTP) (T32 GM07347 to the Vanderbilt University School of Medicine). J. A. S. was supported by the National Science Foundation Graduate Research Fellowships Program (NSF-GRFP). A. E. L. was supported by the 2025 Vanderbilt University School of Engineering Summer Program (VUSRP).

References

1 M. Motwani, S. Pesiridis and K. A. Fitzgerald, *Nat. Rev. Genet.*, 2019, **20**, 657–674.
2 L. Sun, J. Wu, F. Du, X. Chen and Z. J. Chen, *Science*, 2013, **339**, 786–791.
3 M. Shen, X. Jiang, Q. Peng, L. Oyang, Z. Ren, J. Wang, M. Peng, Y. Zhou, X. Deng and Q. Liao, *J. Hematol. Oncol.*, 2025, **18**, 40.
4 B. A. Flood, E. F. Higgs, S. Li, J. J. Luke and T. F. Gajewski, *Immunol. Rev.*, 2019, **290**, 24.
5 M. B. Fuertes, S. R. Woo, B. Burnett, Y. X. Fu and T. F. Gajewski, *Trends Immunol.*, 2013, **34**, 67–73.
6 N. Samson and A. Ablasser, *Nat. Cancer*, 2022, **3**, 1452–1463.
7 J. Yang, Z. Luo, J. Ma, Y. Wang and N. Cheng, *J. Controlled Release*, 2024, **371**, 273–287.
8 B. S. Pan, S. A. Perera, J. A. Piesvaux, J. P. Presland, G. K. Schroeder, J. N. Cumming, B. Wesley Trotter, M. D. Altman, A. V. Buevich, B. Cash, S. Cemerski, W. Chang, Y. Chen, P. J. Dandliker, G. Feng, A. Haidle, T. Henderson, J. Jewell, I. Kariv, I. Knemeyer, J. Kopinja, B. M. Lacey, J. Laskey, C. A. Lesburg, R. Liang, B. J. Long, M. Lu, Y. Ma, E. C. Minnihan, G. O'Donnell, R. Otte, L. Price, L. Rakhilina, B. Sauvagnat, S. Sharma, S. Tyagarajan, H. Woo, D. F. Wyss, S. Xu, D. J. Bennett and G. H. Addona, *Science*, 2020, **369**(6506), 993–999.
9 Q. Xu, J. Xing, S. Wang, H. Peng and Y. Liu, *Heliyon*, 2024, **10**, e33093.
10 H. Luo, T. Tian, C. Hu and F. Hao, *Front. Pharmacol.*, 2025, **16**, 1597443.
11 F. Chen, T. Li, H. Zhang, M. Saeed, X. Liu, L. Huang, X. Wang, J. Gao, B. Hou, Y. Lai, C. Ding, Z. Xu, Z. Xie, M. Luo and H. Yu, *Adv. Mater.*, 2023, **35**(10), 2209919.
12 Y. Liu and F. Pu, *Front. Immunol.*, 2023, **14**, 1254915.
13 J. Zhou, Z. Zhuang, J. Li and Z. Feng, *Int. J. Mol. Sci.*, 2023, **24**, 13316.
14 X. Luo, H. Li, L. Ma, J. Zhou, X. Guo, S. L. Woo, Y. Pei, L. R. Knight, M. Deveau, Y. Chen, X. Qian, X. Xiao, Q. Li, X. Chen, Y. Huo, K. McDaniel, H. Francis, S. Glaser, F. Meng, G. Alpini and C. Wu, *Gastroenterology*, 2018, **155**, 1971–1984.e4.
15 W. He, X. Mu, X. Wu, Y. Liu, J. Deng, Y. Liu, F. Han and X. Nie, *Burns Trauma*, 2024, **12**, tkad050.
16 S. Das, S. Dey, S. Patra, A. Bera, T. Ghosh, B. Prasad, K. D. Sayala, K. Maji, A. Bedi and S. Debnath, *Biomolecules*, 2023, **13**, 1723.
17 M. J. Fuchter, *J. Med. Chem.*, 2020, **63**, 11436–11447.
18 S. E. Caldwell, C. P. Janosko and A. Deiters, *Org. Biomol. Chem.*, 2023, **22**, 302–308.
19 G. Huang, C. Li, J. Si, Y. Cao, M. Zheng, Y. Xue, Q. Zhou, Z. Ge and Y. Ji, *Theranostics*, 2025, **15**, 3979–3994.
20 D. Liu, B. Yu, X. Guan, B. Song, H. Pan, R. Wang, X. Feng, L. Pan, H. Huang, Z. Wang, H. Wu, Z. Qiu, Z. Li and J. Bian, *Chem. Sci.*, 2023, **14**, 4174–4182.
21 C. Ding, M. Du, Z. Xiong, X. Wang, H. Li, E. He, H. Li, Y. Dang, Q. Lu, S. Li, R. Xiao, Z. Xu, L. Jing, L. Deng, X. Wang, M. Geng, Z. Xie and A. Zhang, *Chem. Sci.*, 2023, **14**, 5956–5964.
22 Y. Dou, R. Chen, S. Liu, Y. T. Lee, J. Jing, X. Liu, Y. Ke, R. Wang, Y. Zhou and Y. Huang, *Nat. Commun.*, 2023, **14**(1), 5461.
23 O. I. Gusliakova, L. V. Mikhailova, O. A. Inozemtseva, P. Pidenko, K. Presnyakov, N. A. Shushunova, V. Gulinyan, O. A. Mayorova, O. A. Sindeeva, B. N. Khlebtsov, M. O. Durymanov, M. V. Zyuzin and G. B. Sukhorukov, *Biomater. Adv.*, 2026, **181**, 214632.
24 J. Lee, S. Lee, G. Jo, E. Hwang, J. Lee, J. Han and H. S. Jung, *Molecules*, 2025, **30**, 1587.
25 H. Li, J. Wang, L. Jiao and E. Hao, *Chem. Commun.*, 2024, **5770**, 5770.
26 Y. Cai, T. Chai, W. Nguyen, J. Liu, E. Xiao, X. Ran, Y. Ran, D. Du, W. Chen and X. Chen, *Signal Transduction Targeted Ther.*, 2025, **10**, 115.
27 M. Sadowska, J. Narbutt and A. Lesiak, *Life*, 2021, **11**, 670.
28 P. Kaur and K. Singh, *J. Mater. Chem. C Mater.*, 2019, **7**, 11361–11405.
29 M. C. Malacarne, M. B. Gariboldi and E. Caruso, *Int. J. Mol. Sci.*, 2022, **23**, 10198.
30 T. Yogo, Y. Urano, Y. Ishitsuka, F. Maniwa and T. Nagano, *J. Am. Chem. Soc.*, 2005, **127**, 12162–12163.
31 Y. Xu, S. Lin, R. He, Y. Zhang, Q. Gao, D. Ng and J. Geng, *Chem. Eur. J.*, 2021, **27**(44), 11268–11272.
32 J. A. Peterson, C. Wijesooriya, E. J. Gehrmann, K. M. Mahoney, P. P. Goswami, T. R. Albright, A. Syed, A. S. Dutton, E. A. Smith and A. H. Winter, *J. Am. Chem. Soc.*, 2018, **140**, 7343–7346.
33 T. Slanina, P. Shrestha, E. Palao, D. Kand, J. A. Peterson, A. S. Dutton, N. Rubinstein, R. Weinstain, A. H. Winter and P. Klán, *J. Am. Chem. Soc.*, 2017, **139**, 15168–15175.
34 N. P. Toupin, K. Arora, P. Shrestha, J. A. Peterson, L. J. Fischer, E. Rajagurubandara, I. Podgorski, A. H. Winter and J. J. Kodanko, *ACS Chem. Biol.*, 2019, **14**, 2833–2840.
35 C. Ding, M. Du, Z. Xiong, X. Wang, H. Li, E. He, H. Li, Y. Dang, Q. Lu, S. Li, R. Xiao, Z. Xu, L. Jing, L. Deng, X. Wang, M. Geng, Z. Xie and A. Zhang, *Chem. Sci.*, 2023, **14**, 5956–5964.

36 D. Liu, B. Yu, X. Guan, B. Song, H. Pan, R. Wang, X. Feng, L. Pan, H. Huang, Z. Wang, H. Wu, Z. Qiu, Z. Li and J. Bian, *Chem. Sci.*, 2023, **14**, 4174–4182.
37 Y. Liu, T. Wang and W. Wang, *Chem. Soc. Rev.*, 2025, **54**, 5792–5835.
38 J. Ni, Y. Wang, H. Zhang, J. Z. Sun and B. Z. Tang, *Molecules*, 2021, **26**, 268.
39 G. Stark, *J. Membr. Biol.*, 2005, **205**, 1–16.
40 M. Price, S. R. Terlecky and D. Kessel, *Photochem. Photobiol.*, 2009, **85**, 1491.
41 Z. Zhou, J. Song, L. Nie and X. Chen, *Chem. Soc. Rev.*, 2016, **45**, 6597–6626.
42 X. An, W. Yu, J. Liu, D. Tang, L. Yang and X. Chen, *Cell Death Dis.*, 2024, **15**, 556.